

# Exclusive production of hadron pairs in two-photon interactions

B.Echenard on behalf of the L3 Collaboration

DPNC, University of Geneva, 24 Quai Ernest-Ansermet, CH-1211 Geneva 4, Switzerland  
e-mail: [bertrand.echenard@cern.ch](mailto:bertrand.echenard@cern.ch)

Received: 06 October 2003 / Accepted: 10 October 2003 /  
Published Online: 23 October 2003 – © Springer-Verlag / Società Italiana di Fisica 2003

**Abstract.** The knowledge of two-photon processes increased during the last years thanks to the large sample of  $e^+e^- \rightarrow e^+e^-$  hadrons events collected at LEP. Non perturbative QCD phenomena are investigated through the study of exclusive meson and baryon pair production. The cross sections are measured as a function of the  $\gamma\gamma$  center-of-mass energy,  $W_{\gamma\gamma}$ , and the center-of-mass production angle of the hadron,  $\theta^*$ . Exclusive  $\rho^0\rho^0$  and  $\rho^+\rho^-$  production for quasi-real photons are investigated through a spin-parity-helicity analysis. Exclusive  $\rho^0\rho^0$  production is also studied as a function of the photon virtuality  $Q^2$  and compared to recent QCD predictions.

**PACS.** 13.66Bc Hadron production in  $e^+e^-$  interactions

## 1 Exclusive pion and kaon pair production

Based on the hard scattering approach developed by Brodsky and Lepage [1], predictions have been made for the production of meson pairs in two-photon interactions. In this formalism, the process is factorized into a perturbative  $\gamma\gamma \rightarrow q\bar{q}$  amplitude and a non-perturbative part described by the quark distribution functions of the meson. The  $\gamma\gamma \rightarrow \pi^+\pi^-$  and  $\gamma\gamma \rightarrow K^+K^-$  reactions have been studied by the ALEPH Collaboration [2] for  $|\cos\theta^*| < 0.6$ . The shape of the cross sections are well reproduced by the theoretical predictions but the data have a significantly higher normalization, as shown in Fig. 1 for the  $\gamma\gamma \rightarrow \pi^+\pi^-$  reaction. The QCD predictions are calculated using the hard scattering approach with a distribution amplitude set to its asymptotic form [2]. A fit to

the data with a power law function  $AW^{-6}$  gives a value  $A = 200 \pm 40$  for pions and  $A = 220 \pm 40$  for kaons. The ratio  $\sigma(\gamma\gamma \rightarrow K^+K^-)/\sigma(\gamma\gamma \rightarrow \pi^+\pi^-)$  is thus compatible with one, in complete disagreement with the theoretical prediction of 2.2. Another approach, the so called handbag model [4], has been recently proposed to describe meson pair production. In this model, the process amplitude is factorized into a hard  $\gamma\gamma \rightarrow q\bar{q}$  subprocess and form factors describing the soft  $q\bar{q} \rightarrow meson$  transition. Absolute prediction for the  $\gamma\gamma \rightarrow \pi^+\pi^-$  and  $\gamma\gamma \rightarrow K^+K^-$  cross sections are not available, since input data from other channels are needed. However, the ratio  $\sigma(\gamma\gamma \rightarrow K^+K^-)/\sigma(\gamma\gamma \rightarrow \pi^+\pi^-)$  is predicted to be close to one, in agreement with the data. The observed angular distribution is also reproduced by these calculations.

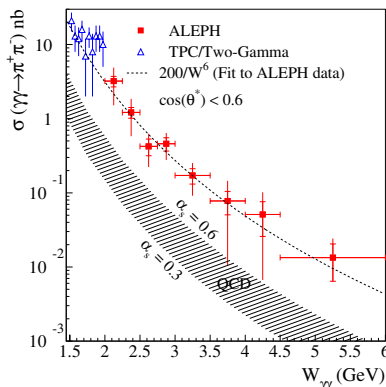


**Fig. 1.** The  $\gamma\gamma \rightarrow \pi^+\pi^-$  cross section as a function of  $W_{\gamma\gamma}$  with the previous measurement of TPC/2 $\gamma$  [3], the QCD prediction and the fit described in the text

## 2 Exclusive baryon pair production

Using the same hard scattering approach, predictions have been made for baryon pair production. However, such calculations with three-quark distribution functions [5,6] failed to reproduce early  $\gamma\gamma \rightarrow p\bar{p}$  measurements [7]. The quark-diquark model [8] was proposed as a possible way to model non-perturbative effects through the use of diquarks, a bound state of two quarks inside the baryon. The handbag model was also adapted to describe baryon pair production [9]. Using flavour symmetry, predictions for the members of the baryon octet can be obtained once the  $\gamma\gamma \rightarrow p\bar{p}$  cross section is measured. The  $\gamma\gamma \rightarrow p\bar{p}$  reaction has been measured as a function of  $W_{\gamma\gamma}$  for  $|\cos\theta^*| < 0.6$  by the L3 [10] and OPAL [11] Collaborations. The calculations of the three-quark model [5] are found to be about an order of magnitude below the measurement, whereas

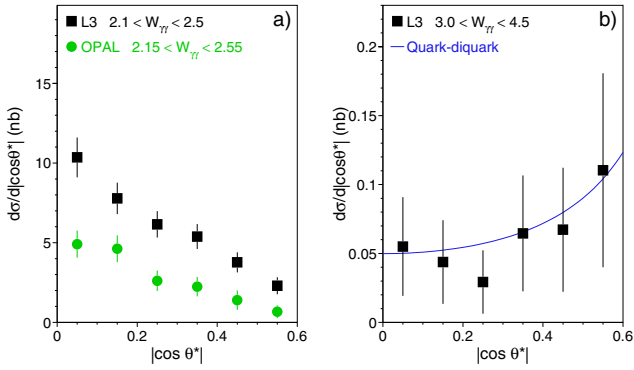


**Fig. 2.** **a** The differential  $\gamma\gamma \rightarrow p\bar{p}$  cross sections as a function of  $|\cos\theta^*|$  for  $2.1 \text{ GeV} < W_{\gamma\gamma} < 2.5 \text{ GeV}$  and **b** for  $3.0 \text{ GeV} < W_{\gamma\gamma} < 4.5 \text{ GeV}$  with the diquark model prediction

the recent quark-diquark predictions [12] describe the data much better. The differential cross sections are also studied in three different mass intervals:  $2.1 \text{ GeV} < W_{\gamma\gamma} < 2.5 \text{ GeV}$ ,  $2.5 \text{ GeV} < W_{\gamma\gamma} < 3 \text{ GeV}$  and  $3 \text{ GeV} < W_{\gamma\gamma} < 4.5 \text{ GeV}$ . The low mass and high mass distributions are displayed in Fig. 2 as example. A distinctive difference is observed between the three distributions. No prediction is available for the quark-diquark model below  $2.5 \text{ GeV}$ , but the data in this region have a qualitatively different behaviour to the diquark prediction above  $W_{\gamma\gamma} = 3 \text{ GeV}$ , as it is strongly peaked at large angles. The intermediate region exhibits a rather flat dependence, which partially agrees with the model predictions. The forward peaking behaviour of the differential cross section in the high mass interval is well reproduced by the quark-diquark model.

The  $\gamma\gamma \rightarrow \Lambda\bar{\Lambda}$ ,  $\gamma\gamma \rightarrow \Lambda\bar{\Sigma}^0 + \Sigma^0\bar{\Lambda}$  and  $\gamma\gamma \rightarrow \Sigma^0\bar{\Sigma}^0$  reactions have been studied by the L3 Collaboration [13] for  $|\cos\theta^*| < 0.6$ . These reactions are identified by first reconstructing the two decay vertices  $\Lambda \rightarrow p\pi^-$  and  $\bar{\Lambda} \rightarrow \bar{p}\pi^+$ . The  $\Sigma^0$  and  $\bar{\Sigma}^0$  candidates are then reconstructed by combining the selected  $\Lambda$  and  $\bar{\Lambda}$  with photons. A maximum likelihood fit, taking the misidentification probabilities between processes into account, is performed to separate the  $\Lambda\bar{\Lambda}$ ,  $\Lambda\bar{\Sigma}^0 + \bar{\Lambda}\Sigma^0$  and  $\Sigma^0\bar{\Sigma}^0$  final states. As the  $\Lambda\bar{\Sigma}^0 + \bar{\Lambda}\Sigma^0$  fraction is found to be negligible, the fit is repeated using only the  $\Lambda\bar{\Lambda}$  and  $\Sigma^0\bar{\Sigma}^0$  components. The  $\gamma\gamma \rightarrow \Lambda\bar{\Lambda}$  and  $\gamma\gamma \rightarrow \Sigma^0\bar{\Sigma}^0$  measurements are compared to different theoretical predictions in Fig. 3. Both measurements are well reproduced by the recent quark-diquark calculations [12], whereas the three-quark model [5] is clearly excluded. Our data are also in agreement with the handbag model predictions [9] inside the theoretical uncertainties.

### 3 Exclusive $\rho$ meson pair production

Exclusive  $\rho$  meson pair production by quasi-real photons was studied by several experiments [14,15,16]. A prominent feature of the reaction  $\gamma\gamma \rightarrow \rho^0\rho^0$  is the broad cross

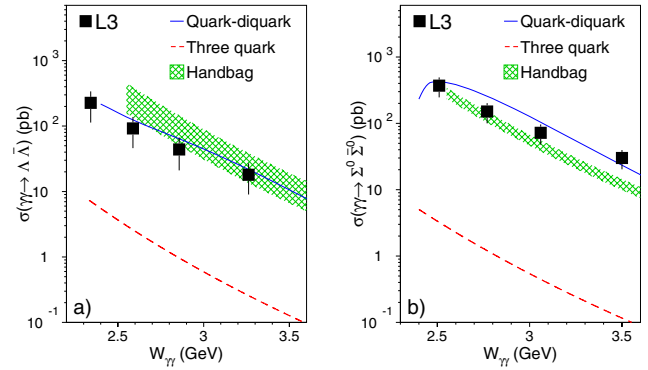


**Fig. 3.** **a** The  $\gamma\gamma \rightarrow \Lambda\bar{\Lambda}$  and **b** the  $\gamma\gamma \rightarrow \Sigma^0\bar{\Sigma}^0$  cross sections as a function of  $W_{\gamma\gamma}$  compared to the three-quark [5], the quark-diquark [12] and the handbag model predictions [9]

section enhancement near threshold, the origin of which is still not well understood. In contrast the cross section for the isospin related reaction  $\rho^+\rho^-$  is shown to be small [17]. On the other hand few data involving highly off-shell virtual photons are available [16], since tagged two-photon processes have a considerably reduced rate. Recent theoretical predictions [18,19] have renewed interest for measuring  $\rho\rho$  production at high  $Q^2$ .

#### 3.1 Exclusive $\rho^0\rho^0$ and $\rho^+\rho^-$ production at $Q^2 \simeq 0$

The  $\gamma\gamma \rightarrow \rho^0\rho^0$  and  $\gamma\gamma \rightarrow \rho^+\rho^-$  reactions at  $Q^2 \simeq 0$  have been studied by the L3 Collaboration via the reactions  $\gamma\gamma \rightarrow \pi^+\pi^-\pi^+\pi^-$  and  $\gamma\gamma \rightarrow \pi^+\pi^0\pi^-\pi^0$ . Following the model proposed by TASSO [14], the signal is modeled with  $\rho\rho$  production in different spin-parity and helicity states ( $J^P, J_z$ ) together with an isotropic production of four pions. All states are assumed to be produced incoherently. The allowed states of a  $\rho\rho$  system in quasi-real  $\gamma\gamma$  reactions are:  $(J^P, J_z) = 0^+, (2^+, 0), (2^+, \pm 2), 0^-$  and  $(2^-, 0)$ . A maximum likelihood fit is used to determine the contributions of the each amplitude. The preliminary results shows a dominance of the  $(J^P, J_z) = (2^+, 2)$  state in both channels. The  $0^+$  and  $0^-$  states give a smaller but non negligible contribution, whereas other states are found to be negligible. A broad enhancement near threshold of the  $\gamma\gamma \rightarrow \rho^0\rho^0$  cross section is observed as in previous measurements and shown in Fig. 4. In contrast, no excess is observed in the  $\rho^+\rho^-$  channel. The cross section ratio  $\sigma(\gamma\gamma \rightarrow \rho^0\rho^0)/\sigma(\gamma\gamma \rightarrow \rho^+\rho^-)$  in the range  $1.2 \text{ GeV} < W_{\gamma\gamma} < 1.6 \text{ GeV}$  is thus incompatible with the hypothesis of a resonance with isospin  $I=0,1$ .

#### 3.2 Exclusive $\rho^0\rho^0$ production at high $Q^2$

Exclusive  $\rho^0\rho^0$  production at high  $Q^2$  has been studied by the L3 Collaboration [20] through the reaction  $e^+e^- \rightarrow \gamma\gamma^* \rightarrow e^+e^-\pi^+\pi^-\pi^+\pi^-$ , where  $\gamma^*$  denotes a virtual photon. Events with four pions a first selected. A maximum likelihood fit using a box method [21] is then performed

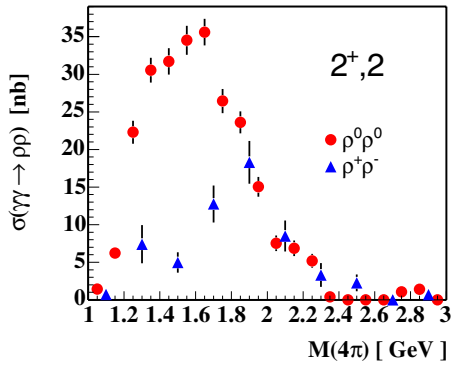


**Fig. 4.** The  $(J^P, J_z) = (2^+, 2)$  component of the  $\gamma\gamma \rightarrow \rho^0\rho^0$  and  $\gamma\gamma \rightarrow \rho^+\rho^-$  cross sections

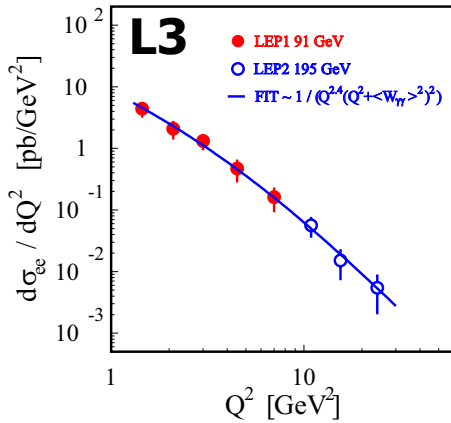


**Fig. 5.** The differential cross section  $d\sigma(e^+e^- \rightarrow e^+e^-\rho^0\rho^0)/dQ^2$  with the fit described in text

for each  $W_{\gamma\gamma}$  and  $Q^2$  interval to determine the number of  $\rho^0\rho^0$  events. The following non-interfering contributions are considered in the fit:  $\gamma\gamma^* \rightarrow \rho^0\rho^0$ ,  $\gamma\gamma^* \rightarrow \rho^0\pi^+\pi^-$  and  $\gamma\gamma^* \rightarrow \pi^+\pi^-\pi^+\pi^-$ . The broad enhancement in the  $\rho^0\rho^0$  cross section near threshold at  $Q^2 \simeq 0$  is also visible in the high  $Q^2$  measurement. The differential cross section  $d\sigma_{ee}/dQ^2$  is plotted in Fig. 5 together with the result of a fit to a form expected from QCD-based calculations:

$$d\sigma_{ee}/dQ^2 \propto Q^{-n}(Q^2 + \langle W_{\gamma\gamma} \rangle^2)^{-2}$$

with  $\langle W_{\gamma\gamma} \rangle = 1.945$ . The fit provides a good description of the  $Q^2$  dependence of the data and gives an exponent  $n = 2.4 \pm 0.3$ , to be compared to the expected value  $n = 2$ . The  $Q^2$  dependence, including the point at  $Q^2 \simeq 0$ , is also well described by a GVDM form factor [22] whereas a steeper decrease, excluded by the data, is expected for a simple  $\rho$ -pole form factor, as shown in Fig. 6.

## Acknowledgments

We would like to thank C.F. Berger, W. Schweiger, M. Diehl and O. Teryaev for very useful discussions.

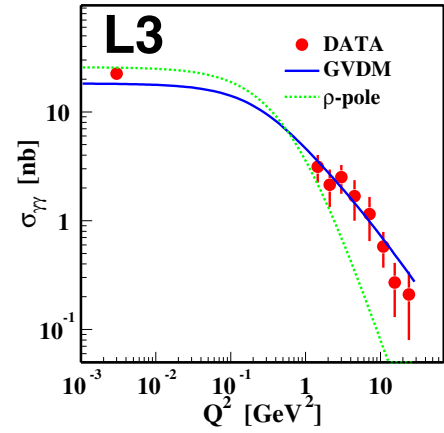


**Fig. 6.** The  $\gamma\gamma^* \rightarrow \rho^0\rho^0$  cross section as a function of  $Q^2$  fitted with a GVDM form factor (solid line) and a  $\rho$ -pole form factor (dotted line)

## References

1. S.J. Brodsky and J.P. Lepage: Phys. Rev. D **22**, 2157 (1980)
2. ALEPH Coll., A. Heister et al.: Nucl. Phys. B **569**, 140 (2003)
3. TPC/2 $\gamma$  Coll., A. Aihara et al.: Phys. Rev. Lett. **57**, 404 (1986)
4. M. Diehl, P. Kroll, and C. Vogt: Phys. Lett. B **532**, 99 (2002)
5. G. Farrar, E. Maina, and F. Neri: Nucl. Phys. B **259**, 702 (1985); Nucl. Phys. B **263**, 746 (1986)
6. D. Millers and J.F. Gunion: Phys. Rev. D **34**, 2657 (1986)
7. ARGUS, H. Albrecht et al.: Z. Phys. C **42**, 543 (1989) and references therein
8. M. Anselmino et al.: Int. Jour. Mod. Phys. A **4**, 5213 (1989)
9. M. Diehl, P. Kroll, and C. Vogt: Eur. Phys. J. C **26**, 567 (2003)
10. L3 Coll., P. Achard et al.: CERN-EP/2003-013
11. OPAL Coll., G. Abbiendi et al.: Eur. Phys. J. C **28**, (2003) 45
12. C.F. Berger, B. Lechner, and W. Schweiger: Fizika B **8**, 371 (1999); C.F. Berger and W. Schweiger: hep-ph/0212066
13. L3 Coll., P. Achard et al.: Phys. Lett. B **536**, 24 (2002)
14. TASSO Coll., M. Althoff et al.: Z. Phys. C **16**, 13 (1982)
15. ARGUS Coll., H. Albrecht et al.: Z. Phys. C **50**, 1 (1991) and references therein
16. PLUTO Coll., C. Berger et al.: Z. Phys. C **38**, 521 (1988); TPC/2 $\gamma$  Coll., H. Aihara et al.: Phys. Rev. D **37**, 28 (1988); TASSO Coll., W. Braunschweig et al.: Z. Phys. C **41**, 353 (1988)
17. ARGUS Coll., H. Albrecht et al.: Phys. Lett. B **217**, 217 (1989) Phys. Lett. B **267** (1991) 535.
18. M. Diehl, T. Gousset, and B. Pire: Phys. Rev. D **62**, (2000) 073014
19. I.V. Anikin, B. Pire, and O.V. Teryaev, hep-ph/0307059
20. L3 Coll., P. Achard et al.: CERN-EP/2003-020
21. D.M. Schmidt, R.J. Morrison, and M.S. Witherell: Nucl. Instr. Meth. A **328**, 547 (1993)
22. J.J. Sakurai and D. Schildknecht: Phys. Lett. B **40**, 121 (1972)